



## Mucosal and systemic physiological changes underscore the welfare risks of environmental hydrogen sulphide in post-smolt Atlantic salmon (*Salmo salar*)

Lazado, Carlo C.; Stiller, Kevin T.; Timmerhaus, Gerrit; Megård-Reiten, Britt-Kristin; Nicolaysen, Ilona Lorraine; Carletto, Danilo; Alipio, Hanna Ross D.; Bergstedt, Julie Hansen; Andersen, Øivind

*Published in:*  
Ecotoxicology and Environmental Safety

*Link to article, DOI:*  
[10.1016/j.ecoenv.2023.115897](https://doi.org/10.1016/j.ecoenv.2023.115897)

*Publication date:*  
2024

*Document Version*  
Publisher's PDF, also known as Version of record

[Link back to DTU Orbit](#)

*Citation (APA):*  
Lazado, C. C., Stiller, K. T., Timmerhaus, G., Megård-Reiten, B-K., Nicolaysen, I. L., Carletto, D., Alipio, H. R. D., Bergstedt, J. H., & Andersen, Ø. (2024). Mucosal and systemic physiological changes underscore the welfare risks of environmental hydrogen sulphide in post-smolt Atlantic salmon (*Salmo salar*). *Ecotoxicology and Environmental Safety*, 270, Article 115897. <https://doi.org/10.1016/j.ecoenv.2023.115897>

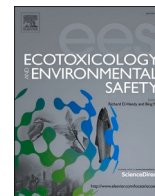
---

### General rights

Copyright and moral rights for the publications made accessible in the public portal are retained by the authors and/or other copyright owners and it is a condition of accessing publications that users recognise and abide by the legal requirements associated with these rights.

- Users may download and print one copy of any publication from the public portal for the purpose of private study or research.
- You may not further distribute the material or use it for any profit-making activity or commercial gain
- You may freely distribute the URL identifying the publication in the public portal

If you believe that this document breaches copyright please contact us providing details, and we will remove access to the work immediately and investigate your claim.



# Mucosal and systemic physiological changes underscore the welfare risks of environmental hydrogen sulphide in post-smolt Atlantic salmon (*Salmo salar*)

Carlo C. Lazado<sup>a,\*</sup>, Kevin T. Stiller<sup>b</sup>, Gerrit Timmerhaus<sup>a</sup>, Britt Kristin Megård Reiten<sup>b</sup>, Ilona Lorraine Nicolaysen<sup>a</sup>, Danilo Carletto<sup>a</sup>, Hanna Ross D. Alipio<sup>a</sup>, Julie Hansen Bergstedt<sup>c</sup>, Øivind Andersen<sup>a</sup>

<sup>a</sup> Nofima, The Norwegian Institute of Food, Fisheries and Aquaculture Research, Ås 1430, Norway

<sup>b</sup> Nofima, The Norwegian Institute of Food, Fisheries and Aquaculture Research, Sunndalsøra 6600, Norway

<sup>c</sup> Technical University of Denmark, DTU Aqua, Section for Aquaculture, The North Sea Research Centre, PO Box 101, Hirtshals 9850, Denmark

## ARTICLE INFO

Edited by Yong Liang

### Keywords:

Aquaculture  
Fish health  
Metabolomics  
Mucosal health  
Nasal immunity  
Recirculating aquaculture system

## ABSTRACT

Atlantic salmon (*Salmo salar*) might encounter toxic hydrogen sulphide (H<sub>2</sub>S) gas during aquaculture production. Exposure to this gas can be acute or chronic, with heightened levels often linked to significant mortality rates. Despite its recognised toxicity, our understanding of the physiological implications of H<sub>2</sub>S on salmon remains limited. This report details the mucosal and systemic physiological consequences in post-smolt salmon reared in brackish water at 12 ppt after prolonged exposure to elevated H<sub>2</sub>S levels over 4 weeks. The fish were subjected to two concentrations of H<sub>2</sub>S: 1 µg/L (low group) and 5 µg/L (high group). An unexposed group at 0 µg/L served as the control. Both groups exposed to H<sub>2</sub>S exhibited incremental mortality, with cumulative mortality rates of 4.7 % and 16 % for the low and high groups, respectively. Production performance, including weight and condition factors, were reduced in the H<sub>2</sub>S-exposed groups, particularly in the high group. Mucosal response of the olfactory organ revealed higher tissue damage scores in the H<sub>2</sub>S-exposed groups, albeit only at week 4. The high group displayed pronounced features such as increased mucus cell density and oedema-like vacuoles. Transcriptome analysis of the olfactory organ unveiled that the effects of H<sub>2</sub>S were more prominent at week 4, with the high group experiencing a greater magnitude of change than the low group. Genes associated with the extracellular matrix were predominantly downregulated, while the upregulated genes primarily pertained to immune response. H<sub>2</sub>S-induced alterations in the metabolome were more substantial in plasma than skin mucus. Furthermore, the number of differentially affected circulating metabolites was higher in the low group compared to the high group. Five core pathways were significantly impacted by H<sub>2</sub>S regardless of concentration, including the phenylalanine, tyrosine, and tryptophan biosynthesis. The plasma levels of phenylalanine and tyrosine were reduced following exposure to H<sub>2</sub>S. While there was a discernible distinction in the skin mucus metabolomes among the three treatment groups, only one metabolite – 4-hydroxyproline – was significantly impacted by H<sub>2</sub>S. Furthermore, this metabolite was significantly reduced in the plasma and skin mucus of H<sub>2</sub>S-exposed fish. This study underscores that prolonged exposure to H<sub>2</sub>S, even at concentrations previously deemed sub-lethal, has discernible physiological implications that manifest across various organisational levels. Given these findings, prolonged exposure to H<sub>2</sub>S poses a welfare risk, and thus, its presence must be maintained at low levels (<1 µg/L) in salmon land-based rearing systems.

## 1. Introduction

Atlantic salmon (*S. salar*) aquaculture stands out as one of the most intensive and technologically advanced fish farming industries on a

global scale. In recent times, a notable innovation in this industry has been the adoption of recirculating aquaculture systems (RAS), largely propelled by the endeavour to transition smolt production to land-based facilities (Bjørndal and Tusvik, 2019; Lazado and Good, 2021). As closed

\* Corresponding author.

E-mail address: [carlolazado@nofima.no](mailto:carlolazado@nofima.no) (C.C. Lazado).

<https://doi.org/10.1016/j.ecoenv.2023.115897>

Received 1 September 2023; Received in revised form 20 December 2023; Accepted 26 December 2023

Available online 4 January 2024

0147-6513/© 2023 The Author(s). Published by Elsevier Inc. This is an open access article under the CC BY license (<http://creativecommons.org/licenses/by/4.0/>).

systems, RAS environments offer various advantages over traditional flow-through systems. These include heightened biosecurity measures, reduced site limitations, optimised water resource utilisation, diminished effluent generation, and enhanced control over environmental conditions, among other benefits (Ahmed and Turchini, 2021; Badiola et al., 2012).

Nonetheless, instances of acute mass mortality have emerged in Norwegian salmon RAS farms in recent years, with these events being correlated to the toxic gas hydrogen sulphide ( $\text{H}_2\text{S}$ ) (Alipio et al., 2023; Rojas-Tirado et al., 2021). This predicament warrants special attention within the context of marine (brackish water and seawater) land-based RAS (Rojas-Tirado et al., 2021) that could likely be attributed to the higher prevalence of sulphate, a key driver of  $\text{H}_2\text{S}$  production (Lételier-Gordo et al., 2020). While  $\text{H}_2\text{S}$  formation can also transpire in freshwater systems, the salinity factor significantly heightens the risk within saline systems (Lételier-Gordo et al., 2020; Rojas-Tirado et al., 2021).

RAS can accommodate microcosms ranging from simple to highly intricate microbial ecosystems, contingent upon the system's maturity. Environmental  $\text{H}_2\text{S}$  arises from microbial activities emanating from the conversion of sulphate by sulphate-reducing bacteria (SRBs) (Harada et al., 1994; Muyzer and Stams, 2008). Recent findings have implicated novel and uncharacterised microbial groups in this process (Lételier-Gordo et al., 2020). SRBs use sulphate ( $\text{SO}_4^{2-}$ ) as a terminal electron acceptor, consequently generating  $\text{H}_2\text{S}$  as a metabolic byproduct (Harada et al., 1994).

Various focal points within a RAS have been pinpointed as primary  $\text{H}_2\text{S}$  sources, including biofilms, sediments, and wastes/sludge. Frequently, these microenvironments foster suboxic-anoxic conditions, propelling the initiation of microbial organic material decomposition, a process leading to  $\text{H}_2\text{S}$  production (Lételier-Gordo et al., 2020; Rojas-Tirado et al., 2021). In an aqueous solution, sulphide exist as one of three species: the gaseous form  $\text{H}_2\text{S}$  or one of two ionic forms, hydrosulphide ( $\text{HS}^-$ ) or sulphide ( $\text{S}^{2-}$ ). It is important to note that the gaseous  $\text{H}_2\text{S}$  variant is associated with toxic effects (Smith et al., 1977).

Even within the micromolar range,  $\text{H}_2\text{S}$  exerts a high toxicity toward most fish species (Bagarinao, 1992; Reynolds, 1976). The vulnerability of fish to  $\text{H}_2\text{S}$  toxicity hinges on their evolutionary adaptations specific to habitat, size, and life stage. Acute exposure to concentrations ranging from 0.25 to 53  $\mu\text{M}$  (ca 8.5–1 806.5  $\mu\text{g/L}$   $\text{H}_2\text{S}$ ) has been identified for numerous fish species as the concentration that is lethal to 50 % of the exposed fish (LC50) (Bagarinao and Vetter (1989); Smith Jr and Oseid (1974). Given the normative circumstances wherein salmon are not consistently subjected to heightened  $\text{H}_2\text{S}$  levels, it is logical to anticipate that critical thresholds are lower. Recently, the critical  $\text{H}_2\text{S}$  concentration ( $\text{H}_2\text{S}_{\text{crit}}$ ), denoting the point at which oxygen uptake falls below the standard metabolic rate or equilibrium is lost, was determined for salmon post-smolts (33 ppt) at  $1.78 \pm 0.39 \mu\text{M}$   $\text{H}_2\text{S}$  (ca 60.7  $\mu\text{g/L}$   $\text{H}_2\text{S}$ ) (Bergstedt and Skov, 2023). This value was particularly lower than previously reported concentrations that salmon could endure over extended periods (Kierner et al., 1995).

Acute exposure to  $\text{H}_2\text{S}$  has discernible impacts on the mucosal defences of salmon smolts, with particular emphasis on the olfactory organ and gills, both exhibiting heightened responsiveness indicated by modifications in gene expression and histological characteristics (Alipio et al., 2023). Notably, *in vitro* models have demonstrated that sulphide donors can modify the immunological status of nasal leukocytes (Cabillon and Lazado, 2022) while also interfering with the detoxification functions within olfactory rosette explants of salmon (Alipio et al., 2022). The susceptibility of the olfactory organ of salmon to  $\text{H}_2\text{S}$  is consistent with earlier findings in mammals, indicating that  $\text{H}_2\text{S}$  functions as a contact irritant and can trigger injury to nasal respiratory epithelia, even resulting in bleeding from the nose, pharynx, gums, tongue, trachea, and bronchi (Mousa, 2015; Roberts et al., 2008).

The effects of acute  $\text{H}_2\text{S}$  exposure on salmon have been further elucidated through metabolomics. This analysis unveiled more

pronounced alterations in the metabolite profile of skin mucus compared to blood. Modified pathways encompass tRNA charging, the branched-chain amino acid biosynthesis superpathway, and the biosynthesis of glucosinolates from phenylalanine (Alipio et al., 2023). Although elevated  $\text{H}_2\text{S}$  levels have been linked to fatality, it is important to note that salmon might experience prolonged exposure to sub-lethal levels in RAS (Nicolaysen et al., 2024). The current understanding of physiological changes in salmon during extended  $\text{H}_2\text{S}$  exposure remains limited, primarily due to the predominant focus on mortality outcomes stemming from  $\text{H}_2\text{S}$  exposure.

This study aimed to elucidate the mucosal and systemic physiological consequences caused by prolonged exposure to heightened levels of  $\text{H}_2\text{S}$  in post-smolt Atlantic salmon reared in brackish water RAS. We hypothesised that prolonged exposure to  $\text{H}_2\text{S}$  affects the mucosal barrier functions, resulting in a systemic metabolomic dysregulation thereby affecting the health and welfare of salmon. The concentrations administered during the experiment had previously been documented in routine salmon RAS farm operations and were formerly considered sub-lethal; however, the outcomes of prolonged exposure revealed a contrasting reality. Adopting a brackish water system in this trial holds industry significance, as it represents an economically viable production approach before the eventual transfer of post-smolts to open sea cages (Ytrestøyl et al., 2020).

## 2. Materials and methods

### 2.1. Ethical consideration

The fish experiment complied with the European Union Directive 2010/63/EU and Norway's Animal Welfare Act of 2009. The study received approval from the Norwegian Food Safety Authority under permit number FOTS ID 28927. The key personnel participating in the trial had completed a FELASA C Laboratory Animal Science Course.

### 2.2. Experimental fish

The fish trial was conducted at Nofima's Aquaculture Research Station in Sunndalsøra, Norway. The experimental fish of the Bolaks strain were bred and smoltified on-site at the research station. They were initially reared within a freshwater flow-through system before being utilised in the experiment. The smoltification status of the fish was verified through a visual examination and a seawater test involving exposure to 34 ppt salinity for 72 h, along with the measurement of plasma chloride levels. Successful seawater adaptation was confirmed when the fish could regulate plasma chloride levels to below 150  $\text{mmol L}^{-1}$  during the test.

### 2.3. $\text{H}_2\text{S}$ exposure trial

#### 2.3.1. Description of the experimental RAS unit

The  $\text{H}_2\text{S}$  exposure trial was conducted within a modular RAS unit (Landing Aquaculture, Netherlands) featuring an aggregate RAS water capacity of approximately 1 150 L (Fig. 1A). Each experimental RAS unit incorporated functionalities designed to eliminate solids, particulates, ammonia, and carbon dioxide, along with provisions for oxygenation and precise temperature regulation. A 500 L Cornell dual drain tank was integrated into every unit, linked downstream to a drum filter and a moving bed bioreactor, culminating in a pump sump. Emerging from the sump, the water was routed back to the tank, coursing through an oxygen cone and a chiller. In a parallel circuit, water underwent constant circulation through a  $\text{CO}_2$  degasser. The pump sump was divided to exclusively channel degassed water, ensuring its uptake by the pump for reintegration into the fish tank. The overall water flow maintained a rate of 30 L/min, yielding a hydraulic retention time of 16.7 min

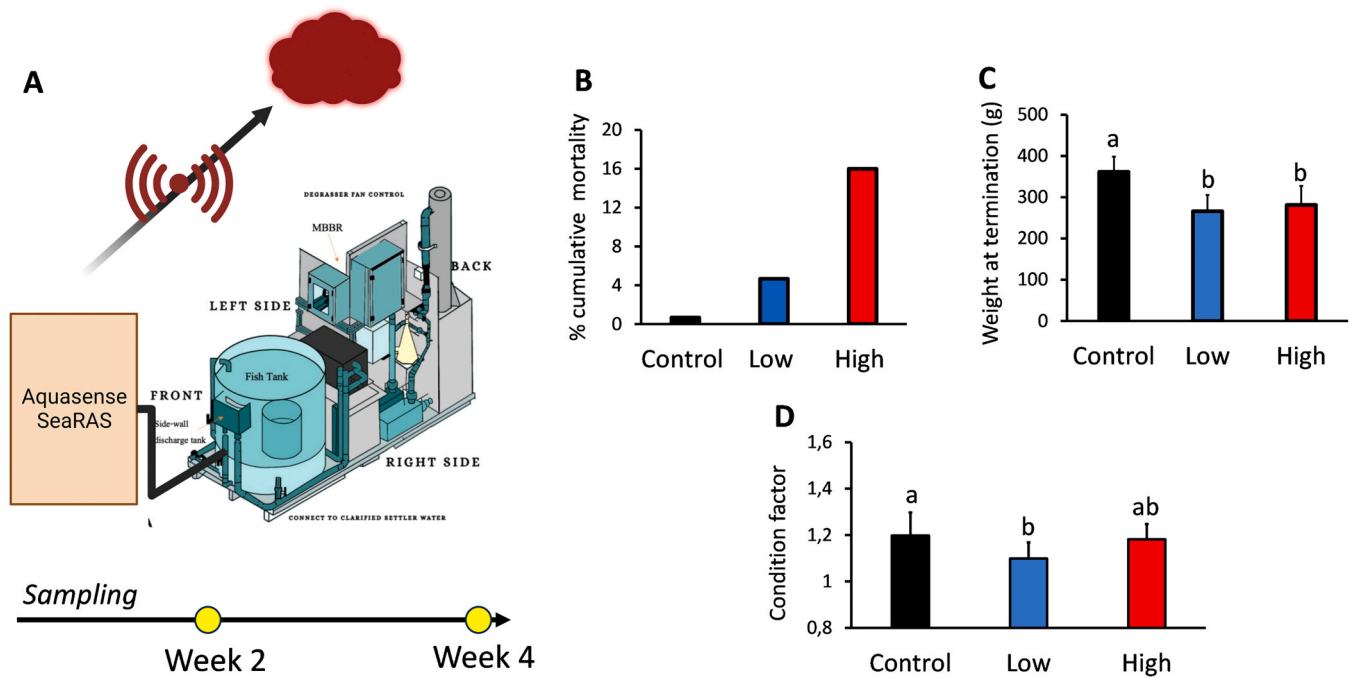


**Fig. 1.** Four-week prolonged H<sub>2</sub>S exposure trial. Sampling was performed in week 2 and week 4. **A)** An illustration of the modular RAS unit used in the study (provided by Per Brunsvik, Nofima). Aquasense SeaRAS sensor was used to monitor the H<sub>2</sub>S level continuously (Lien et al., 2022). Data were transmitted to a cloud database. Background H<sub>2</sub>S level < 0.3 µg/L was recorded in the control group. **B)** Cumulative mortality (%) after a 4-week exposure to H<sub>2</sub>S. **C)** Mean weight and **D)** condition factor of fish exposed to H<sub>2</sub>S taken at week 4. Different letters denote significant differences (P < 0.05).

### 2.3.2. Prolonged exposure to elevated H<sub>2</sub>S

Each unit received a stock of 50 post-smolt salmon weighing an average of  $162 \pm 2.5$  g at the commencement of the trial. The fish were acclimatised for 3 weeks before the continuous introduction of H<sub>2</sub>S into the system began. Throughout the experiment, the rearing conditions remained consistent, encompassing a salinity of 12 ppt, dissolved oxygen levels exceeding 90 % saturation, a temperature set at 12 °C, a pH of 7.7, and a photoperiod of 24-h light:0-h dark cycle. This experimental setup was complemented by a continuous feeding regimen utilising Ewos micro boost 80 feed.

The H<sub>2</sub>S exposure phase spanned 4 weeks, comprising three distinct treatment groups: control (0 µg/L), low (1 µg/L H<sub>2</sub>S), and high (5 µg/L H<sub>2</sub>S). These concentration levels were chosen based on insights gleaned from a preceding monitoring initiative, profiling H<sub>2</sub>S levels within operational RAS farms in Norway (Paulo Fernandes and Åse Åtland, NIVA, personal communication). Three separate replicate modular RAS units represented each of the treatment groups. To introduce H<sub>2</sub>S, a peristaltic pump drew directly from a dosing tank containing sodium hydrosulfide hydrate (NaSHxH<sub>2</sub>O) at a concentration of 1 g/L (Sigma-Aldrich, MO, USA). Given the reactivity of H<sub>2</sub>S, the stock solution was freshly prepared daily. To ensure accurate monitoring, the real-time H<sub>2</sub>S content within the system, including the control group, was measured by the SeaRAS AquaSense sensor (Lien et al., 2022). Dosage adjustments were routinely implemented to uphold the targeted H<sub>2</sub>S levels. Daily records of mortality rates and behavioural observations were kept throughout the experiment. For additional details of the trial, please refer to Nicolaysen et al., 2024.

### 2.3.3. Sample collection

Sampling took place during the second and fourth weeks of H<sub>2</sub>S exposure. Five fish were gently netted from each tank on each sampling occasion and humanely euthanised with an overdose of Finquel (0.5 mg/L, MSD Animal Health, Netherlands) followed by measurements of length and weight. Blood was extracted from the caudal vein using a heparinised vacutainer (BD, NY, USA), with plasma being separated following a 10-minute centrifugation at 3700 rpm using the

Avanti J-15R Centrifuge (Beckman Coulter, CA, USA). The obtained plasma was then stored at -80 °C until analysis. To collect skin mucus samples, the left side beneath the lateral line was swabbed using FLOQSwab® (COPAN Diagnostics, Murrieta, CA, USA), and the samples were promptly snap-frozen in dry ice. Both olfactory organ (rosettes) from each side of the fish were collected for subsequent gene expression analysis and histological examination. The left-side rosette was allocated for microarray analysis, while those on the right was dedicated to histological evaluations. The olfactory organ was the focus of this study because of its role in olfaction (i.e., H<sub>2</sub>S is a dissolved gas with a distinct smell), immunity (i.e., earlier we have shown that the olfactory organ of salmon is sensitive to toxicants in RAS (Lazado et al., 2021; Osório et al., 2022)) and sensitivity to H<sub>2</sub>S (i.e., demonstrated both *in vivo* and *ex vivo* exposure in salmon (Alipio et al., 2022; Alipio et al., 2023; Cabillon and Lazado, 2022)). Preparations for microarray analysis involved suspending the samples in RNeasy lysis buffer (Qiagen, Crawley, UK), maintaining them at 4 °C overnight to facilitate penetration, and storing them at -80 °C until RNA isolation. Meanwhile, histological samples were preserved in 10 % formalin (CellStor, CellPath, UK), with an initial overnight fixation at room temperature. Following fixation, they were transferred to 70 % ethanol and stored at 4 °C until further tissue processing.

### 2.4. Microarray analysis

Total RNA from the olfactory organ (2 fish per replicate tank, 6 fish per treatment group) was isolated using the Agencourt RNAdvance™ Tissue Total RNA Purification Kit (Beckman Coulter Inc., CA, USA). The quantity of RNA was assessed using a Nanodrop, while its quality underwent further assessment via the Agilent® 2100 Bioanalyzer™ RNA 6000 Nano Kit (Agilent Technology Inc., Santa Clara, CA, USA), revealing that all samples achieved an RNA Integrity Number (RIN) exceeding 8. Subsequently, the microarray analysis was conducted utilising a custom-designed 44 K Atlantic salmon DNA oligonucleotide microarray designated SIQ-6 (Agilent Array, ICSASG\_v2), with all reagents sourced from Agilent Technologies. The One-Colour Quick Amp



Labelling Kit facilitated the RNA amplification and Cy3 labelling, employing 110 ng of RNA template per reaction. The Gene Expression Hybridization Kits were employed for RNA fragmentation, followed by a 15-h hybridisation period within a 65 °C oven with a consistent rotational speed of 10 rpm. Following hybridisation, the arrays were methodically washed using Gene Expression Wash Buffers 1 and 2 and subsequently scanned using the Agilent SureScan Microarray Scanner. The pre-processing stage was accomplished within Nofima's bioinformatics software package Salmon and Trout Annotated Reference Sequences (STARS) (Krasnov et al., 2011). The raw data has been submitted to Gene Expression Omnibus (GEO) under accession number GSE246815.

## 2.5. Histological evaluation

The olfactory organ (3 fish per replicate tank, 9 fish per treatment group) was embedded in paraffin, with subsequent sectioning into 5 µm slices. These slices were then positioned onto microscope slides and subjected to overnight heat fixation at 60 °C. An automated stainer (ST5010, Germany) was utilised for Periodic Acid Schiff-Alcian Blue (AB/PAS) staining. The sections underwent digitisation utilising a slide scanner (Aperio CS2, USA).

Tissue damage scoring was executed using a 0-to-3 scale, specially formulated for assessing the impact of H<sub>2</sub>S exposure on salmon olfactory organ (Supplementary File 1). This scoring protocol effectively addresses the characteristic structural alterations often linked to H<sub>2</sub>S exposure. The evaluation process employed a gradient scoring system, where a score of 0 denotes a healthy state characterised by unaltered morphology and minimal structural changes. Conversely, a score of 3 corresponds to severe damage and substantial structural modifications (Alipio et al., 2023). For measurements, the thickness of the olfactory lamellar epithelium was gauged across 5 distinct lamellae per fish, with three random measurements taken from each lamella. A similar methodology was applied to assess the thickness of the *lamina propria*. Additionally, the width of the mucosal tip was quantified using the same lamellae utilised for measuring the lamellar epithelium and *lamina propria* thickness. All these parameters were subject to blind evaluations to mitigate any potential biases.

## 2.6. Metabolomics profiling

Samples obtained during the fourth week were utilised for profiling purposes. Due to limited quantities, skin mucus from three fish within each RAS unit was pooled. Conversely, unpooled samples were earmarked for plasma metabolomics. The extraction of metabolites from skin mucus (20 µl) and plasma (50 µl) involved diluting the matrix using their respective extraction solutions (mucus = mixture of acetonitrile, methanol, and formic acid at a ratio of 1:1:0.01 v/v/v; plasma = acetonitrile and methanol at a ratio of 1:1 v/v). Stable isotope-labelled standards (6 µl) were added to the extracts before passage through a phosphor removal cartridge (Phree, Phenomenex). An aliquot (100 µl) was then transferred into a high-recovery HPLC vial, followed by the gentle removal of the solvent under a flow of nitrogen. Extracts were reconstituted in a mobile phase mixture (100 µl, 10 %B in 90 %A).

The samples were analysed by MS-Omics, utilising a Thermo Scientific Vanquish LC coupled with an Orbitrap Exploris 240 MS (Thermo Fisher Scientific). An electrospray ionisation interface was employed as the ionisation source, and both positive and negative ionisation modes were utilised with polarity switching. The Ultra Performance Liquid Chromatography process was conducted with slight modifications based on prior protocols (Doneanu et al., 2011), which had been adapted for salmon plasma (Lazado et al., 2020) and mucus (Alipio et al., 2023). Compound Discoverer 3.3 (Thermo Scientific) was employed to extract peak areas. Compound identification was executed across four levels: Level 1: Identification based on retention times (compared to in-house authentic standards), accurate mass (within a 3 ppm deviation), and

MS/MS spectra; Level 2a: Identification based on retention times (compared to in-house authentic standards) and accurate mass (within a 3 ppm deviation); Level 2b: Identification based on accurate mass (within a 3 ppm deviation) and MS/MS spectra; and Level 3: Identification based solely on accurate mass (within a 3 ppm deviation). For detailed annotation strategy, kindly refer to **Supplementary File 2**.

## 2.7. Data analyses

SigmaPlot (Systat Software Inc., London, UK) was employed to discern statistical distinctions across treatment groups and time points for both performance parameters (such as weight and condition factor) and various nasal morphometric parameters (including the thickness of the olfactory lamellar epithelium *lamina propria*, and width of the mucosal tip). To ensure the appropriateness of the analysis of variance (ANOVA), prerequisites were assessed, including a Normality Test using the Shapiro-Wilk test and an Equal Variance Test using the Brown-Forsythe test. The performance parameters data underwent one-way ANOVA, while the nasal morphometric data were subjected to a two-way ANOVA. For pairwise multiple comparisons, the Holm-Sidak method was implemented. The categorical data concerning tissue damage scores were evaluated using the Chi-squared test. A significance level of  $P < 0.05$  was deemed the statistical significance threshold.

Regarding the microarray data, an initial filtering process involved the removal of genes featuring three or more missing values, ultimately yielding 34,426 genes for subsequent analysis. For each of these filtered genes, two-way ANOVAs were conducted, with the factors being time point and treatment (conducted in R, version 4.1.1, aov() function of the stats package). Genes displaying differential expression (DEGs) were characterised by at least one two-way ANOVA P-value below 0.05 and a minimum log<sub>2</sub> expression difference greater than the absolute value of 0.8. This resulted in 1979 genes, which were further analysed by calculation of group means (normalized to the mean of the week 2 control group) and subsequent clustering (hclust() function with complete linkage of Euclidean distances, calculated by the dist() function). Subclusters were retrieved by the cutree() function. The subclusters were analyzed for over-representation of functional annotation terms with Fisher-tests (fisher.test() function, alternative set to "greater"). For data visualisation of the cluster the heatmap.2() function from the gplots (version 3.1.3) package was used. Expression values were visualised by custom bar plots, showing the mean expression value of the subclusters with error bars for ± SEM.

An initial step for the metabolomics data involved evaluating normality through the Shapiro-Wilk test, followed by selecting the most appropriate univariate statistical test. If the data exhibited conformity to a normal distribution, t-tests were conducted. Subsequently, data underwent correction using the Benjamini-Hochberg method, with a false positive rate of 0.05 employed. This correction entailed calculating the Benjamini-Hochberg critical value, denoted as (i/m)Q, for each compound, which was subsequently utilised for p-value adjustment. Statistics were done in Python 3.9.12 64-bit | Qt 5.15.2 | PyQt5 5.15.7 | Windows 10 using the statsmodels package on a custom script. PCA plots were prepared in MatLab2023b, using the Eigenvector PLS\_toolbox. Topological pathway analysis was undertaken within MetaboAnalyst 5.0, utilising the Hypergeometric test as enrichment. The relative centrality of the interrelationships was opted for, and the zebrafish (*Danio rerio*) metabolome served as the reference metabolome (Xia et al., 2009). A representative KEGG pathway map was downloaded from KEGG PATHWAY Database (<https://www.genome.jp/kegg/pathway.html>) and metabolites significantly affected were mapped manually. The annotated pathway was constructed in MS Powerpoint.

### 3. Results

#### 3.1. Mortality, production performance and behavioural changes

The mortality in both H<sub>2</sub>S-exposed groups occurred gradually, with the high group recording its first mortality only after the second week of exposure. The control and low groups, on the other hand, experienced their initial mortalities during the 4th week of exposure. Following 4 weeks of exposure, cumulative mortalities reached 4.7 % for the low and 16 % for the high groups (Fig. 1B). Notably, behavioural changes were observed in the H<sub>2</sub>S-exposed groups, particularly in the high group. Prior to mortality documentation, the fish exhibited swimming behaviour following the water current and showed signs of lethargy and exhaustion. Furthermore, certain fish were observed swimming near the water surface and inlet, displaying increased opercular ventilation activity. The H<sub>2</sub>S-exposed groups had a significantly lower mean weight upon termination compared to the control group (Fig. 1C). Specifically, the mean weight of the low and high groups was 26 % and 22 % lower, respectively, than that of the control group. The condition factor of the low group was particularly lower than that of the control group (Fig. 1D). However, there were no significant differences between the condition factors of the two H<sub>2</sub>S-exposed groups.

#### 3.2. Histological changes in the olfactory organ

Tissue damage scores ranged from 0 to 2 across various groups and

time points (Fig. 2A). During week 2, no inter-treatment differences were evident, whereas the low and high groups exhibited significantly higher proportions of higher damage scores than the control group by week 4 (Fig. 2A). A noteworthy temporal shift was only discernible in the low group, where the proportion of score 2 experienced a significant increase at week 4 in comparison to week 2. There were no notable inter-treatment differences in the thickness of the olfactory lamellar epithelium at either sampling point (Fig. 2B). Within the control group, thickness exhibited a significant disparity between week 2 and week 4, with an increase of no less than 10 %. However, this change was not observed within the two H<sub>2</sub>S-exposed groups. Conversely, the thickness of the *lamina propria* displayed no significant changes across treatments and time points (Fig. 2C). The width of the mucosal tip expanded significantly between week 2 and week 4 within the control group, manifesting an increase of at least 32 % (Fig. 2D). This alteration was absent in both the low and high groups. Additionally, no significant inter-treatment differences were detected at either time point.

Fig. 2E and F present illustrative histological sections of the olfactory organ, showcasing the control group (Fig. 2E) and the high group (Fig. 2F). Mucus cells are distributed along the mucosal tip and the epithelial lining of the nasal cavity. A noticeable elevation in mucus cell density was noted in the high group compared to the control group. Furthermore, substantial oedema-like vacuoles were evident in the H<sub>2</sub>S-exposed fish, with their presence detected both at the tip of the olfactory lamella and within the nasal cavity wall.

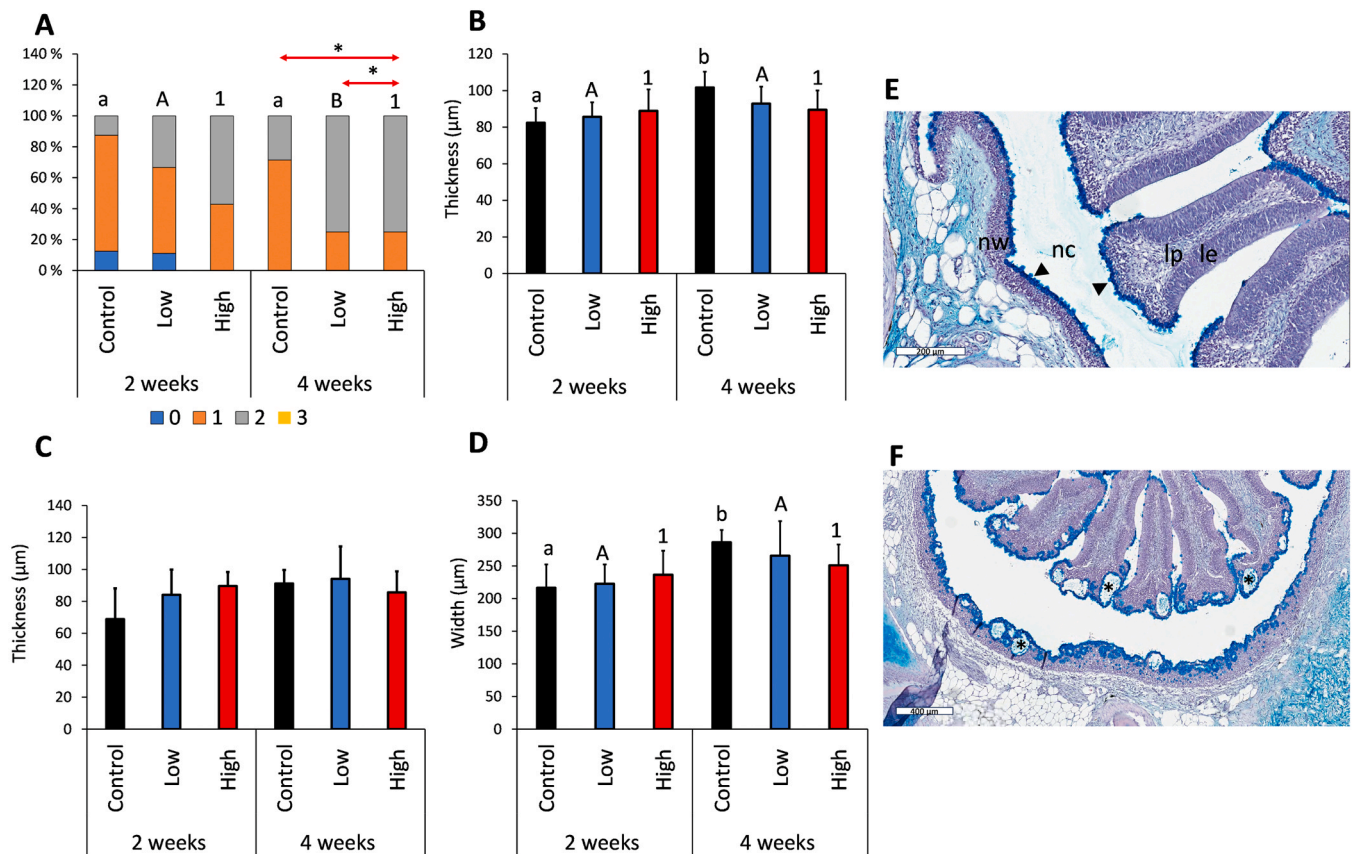


**Fig. 2.** Histological features of the olfactory organ of salmon after prolonged exposure to H<sub>2</sub>S. Nasal parameters such as **A)** tissue damage score, **B)** thickness of olfactory lamellar epithelium, **C)** thickness of *lamina propria*, and **D)** width of the mucosal tip were assessed (n = 9; 3 fish per replicate RAS unit of a treatment group; each treatment group had 3 RAS units). Values are presented as mean ± standard deviation. Differences between time points within a treatment group were denoted by lowercase letters for control, uppercase letters for low and numbers for high. An asterisk (\*) indicated a significant difference between 2 treatment groups (e.g., control versus high group at week 4) in a particular time point. Representative histological sections of the olfactory organ from **E)** control and **F)** high groups, stained with AB/PAS. lp = *lamina propria*; le = lamellar epithelium; nc = nasal cavity; nw = nasal wall; arrow (◄) = dense aggregates of mucus cells; asterisk (\*) = oedema-like vacuoles.

### 3.3. Transcriptomic changes in the olfactory organ

A total of 1979 genes exhibited distinct alterations across various treatments and time points, as depicted in Fig. 3 and detailed in Supplementary File 3. Generally, the extent of change was more pronounced at week 4 than week 2, with particularly notable effects observed within the high group. These genes were organised into seven major clusters, as illustrated in Fig. 3A and B. Clusters 1 and 7 emerged as the two smallest clusters, displaying evident shifts in the H<sub>2</sub>S-exposed groups at week 4. In particular, Cluster 1, primarily encompassing immune effector molecules and angiogenesis-related genes, exhibited downregulation following H<sub>2</sub>S exposure by week 4. Conversely, Cluster 7, comprising genes involved in tissue extracellular matrix (predominantly collagen and mucus), demonstrated upregulation within the high group at week 4.

Cluster 2 emerged as the largest cluster, encompassing 932 genes, and was characterised by a prevalent downregulation response by week 4. Particularly, within the high group, this cluster was inclined towards upregulation at week 2, followed by a substantial downregulation at week 4. Most of these genes were pivotal for maintenance of

extracellular matrix (ECM), steroid metabolism, and immune lectin activity. Cluster 3 mirrored the trend observed in Cluster 2, albeit with a relatively lower gene count. The genes affected within this cluster primarily pertained to collagen-based ECM and cellular transport metabolism.

Cluster 4 exhibited significant upregulation within the high group at week 4. Among the highly affected genes were those associated with viral responses (including viral transcription modules and IFN), immune reactions, and tissue erythrocyte function. Cluster 5 spotlighted genes prominently influenced in the low group at week 4, where those linked to tissue secretion and cell cilia experienced upregulation. Lastly, the expansive Cluster 6 displayed upregulation within the high group at week 4. Noteworthy genes within this cluster included transcription modules for bacteria and viruses, components of the mucus extracellular matrix, and various immune function groups.

### 3.4. Alterations in circulating and mucosal metabolomic profiles

#### 3.4.1. Plasma

1087 compounds were detected in the plasma samples

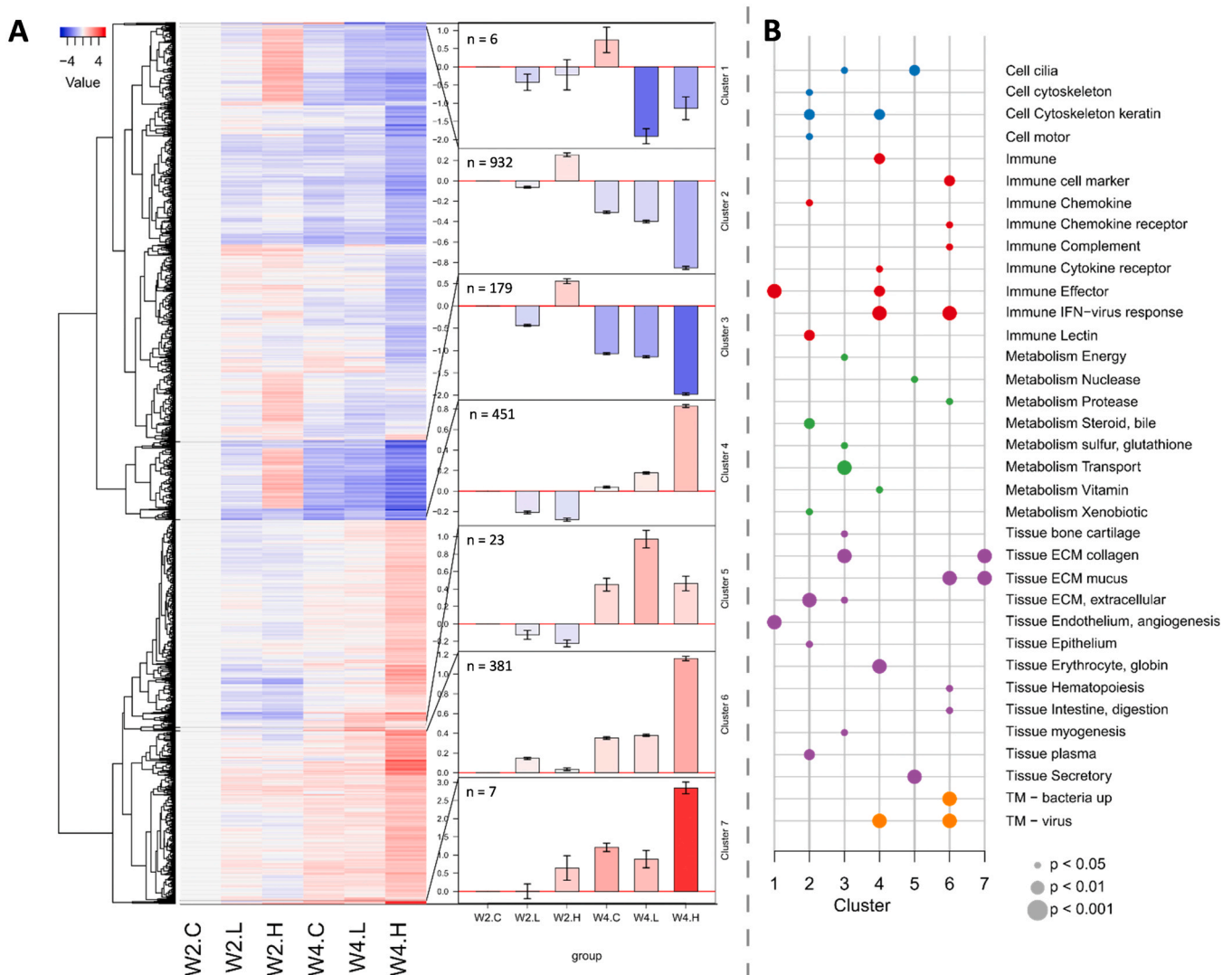


**Fig. 3.** Transcriptomic changes in the olfactory organ of salmon following prolonged exposure to H<sub>2</sub>S. Gene expression analysis was performed at weeks 2 and 4. **A)** The heatmap on the left shows down- and upregulation of DEGs in a colour gradient from blue to red. The dendrogram was split into seven clusters, and the mean values for genes within these clusters are represented in bar plots (error bars show  $\pm$  standard error of the mean) in the centre. **B)** Functional gene categories of the seven clusters. The dot size represents the P-value according to Fischer's Exact Test. (n = 6; 2 fish per replicate RAS unit of a treatment group; each treatment group had 3 RAS units).



(Supplementary File 4). Based on the annotation levels described in Section 2.6, these metabolites were categorised as follows: 44 metabolites at level 1, 64 compounds at level 2a, and 44 compounds at level 2b. With a lower degree of certainty, 280 compounds were annotated based on exact mass, isotope pattern, and reference count, falling under level 3. Additionally, 655 compounds could not be confidently identified and were thus classified as unknown (Fig. 4A).

The score plot derived from a PCA model, calculated on the compounds annotated at levels 1 and 2a within the reduced dataset, is displayed in Fig. 4B. Notably, a discernible separation is evident, with the control group positioned in the lower right quadrant and the H<sub>2</sub>S-exposed groups occupying the upper and lower left quadrants. The loading plot depicted in Fig. 4C elucidates the variables responsible for the observed patterns in the score plot.

A stringent criterion allowed only compounds annotated at levels 1 and 2a to further characterise the modified metabolites. 72 metabolites exhibited significant alterations compared to the control group, as depicted in Fig. 4D. Among these, 21 significantly affected metabolites were exclusively identified in the low group. This subset included compounds such as thiamine, betaine, and guanine. Conversely, nine markedly impacted metabolites were exclusively observed in the high group, featuring adenine, hypoxanthine, and choline.

Furthermore, 42 metabolites displayed significant changes in both

H<sub>2</sub>S groups. This subset encompassed compounds like 4-hydroxyproline, inosine, phenylalanine, carnitine, and threonic acid. To pinpoint biological pathways influenced by H<sub>2</sub>S, irrespective of concentration, our pathway analysis centred on these 42 shared metabolites, as demonstrated in Fig. 4E. Five of these metabolites were distributed across 23 pathways (Supplementary File 3), exhibiting noteworthy alterations. These included pathways associated with Phenylalanine, tyrosine, and tryptophan biosynthesis; Phenylalanine metabolism; Aminoacyl-tRNA biosynthesis; Glycine, serine, and threonine metabolism; Riboflavin metabolism; as well as D-Glutamine and D-glutamate metabolism.

The KEGG pathway about phenylalanine, tyrosine, and tryptophan biosynthesis is depicted in Fig. 5A. Within this pathway, three pivotal metabolites—phenylalanine, tyrosine, and tryptophan – displayed significant alterations due to H<sub>2</sub>S exposure, regardless of concentration. The levels of these metabolites in the plasma were lower than those in the control group. Additionally, both H<sub>2</sub>S-exposed groups exhibited comparable behaviour concerning these metabolites (Fig. 5B and C).

Pathway analysis was also conducted for the modified metabolites exclusive to specific H<sub>2</sub>S-exposed groups (Supplementary File 5). Given the relatively constrained count of metabolites unique to the high group, the analysis was centred on the low group. The 21 significantly altered metabolites exclusive to the low group were distributed across 9 pathways, with five pathways exhibiting noteworthy alterations. Among

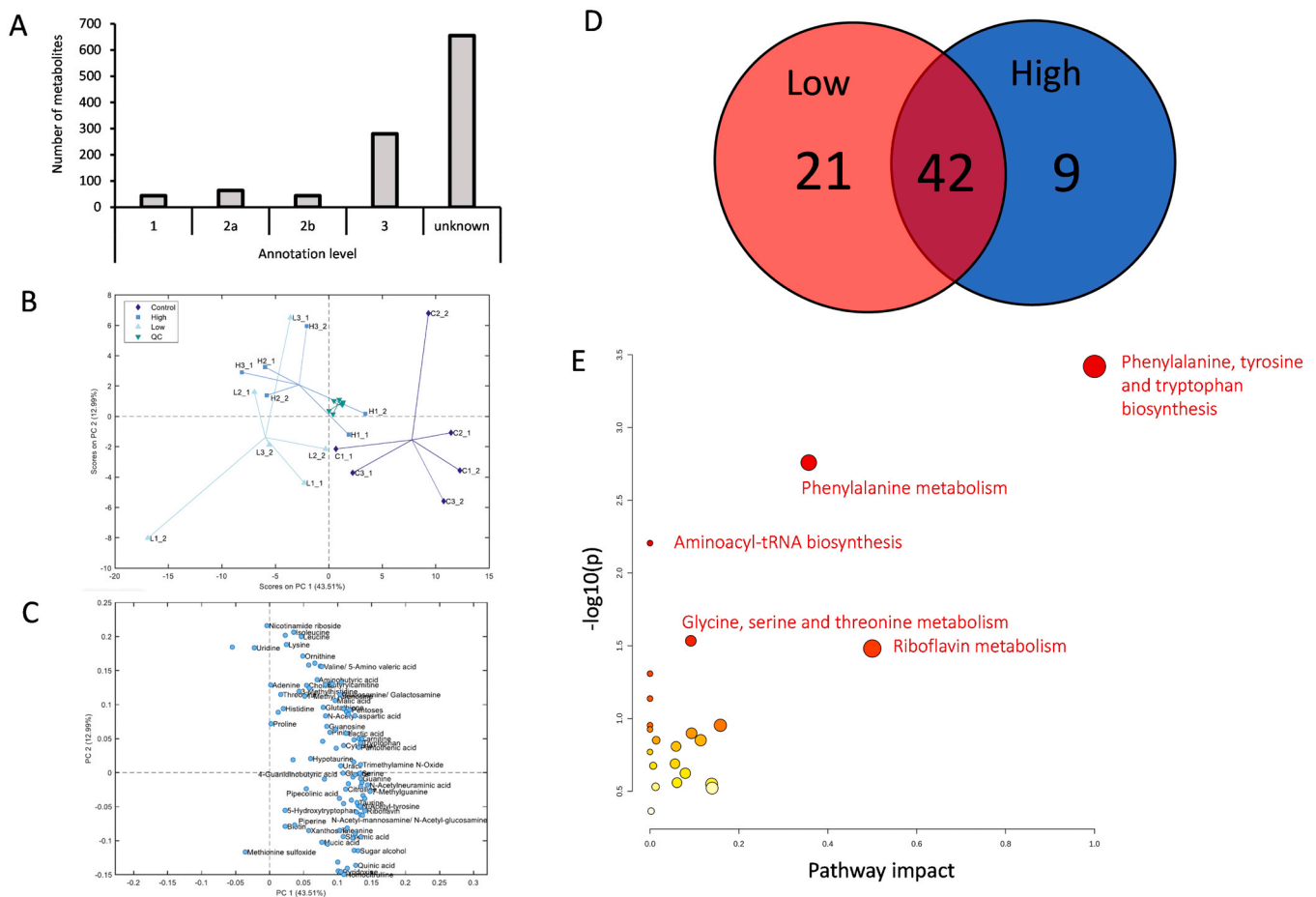


**Fig. 4.** Plasma metabolome of salmon following prolonged exposure to H<sub>2</sub>S. **A)** Metabolites identified in the matrix based on five annotation levels. **B)** Score plot of PC2 over PC1 in the model calculated on the relative concentrations of the variables annotated on levels 1 and 2a in the reduced dataset. Data have been auto-scaled. To ensure high-quality sample preparation, a quality control sample (QC sample) was prepared by pooling small equal aliquots from each sample, to create a representative average of the entire set. This sample was treated and analysed at regular intervals throughout the sequence. **C)** Loading plot from PCA model calculated on the relative concentrations of the variables annotated on levels 1 and 2a in the reduced dataset. Data have been auto-scaled, and overlapping labels were removed to improve readability. **D)** Venn diagram showing the significantly altered metabolites in the low and high groups relative to the control. **E)** Metabolic pathways where the differentially affected metabolites were identified as involved according to topological pathway analyses. Labelled Pathways indicate that the alteration was statistically significant ( $P < 0.05$ ). ( $n = 6$ ; 2 fish per replicate RAS unit of a treatment group; each treatment group had 3 RAS units).

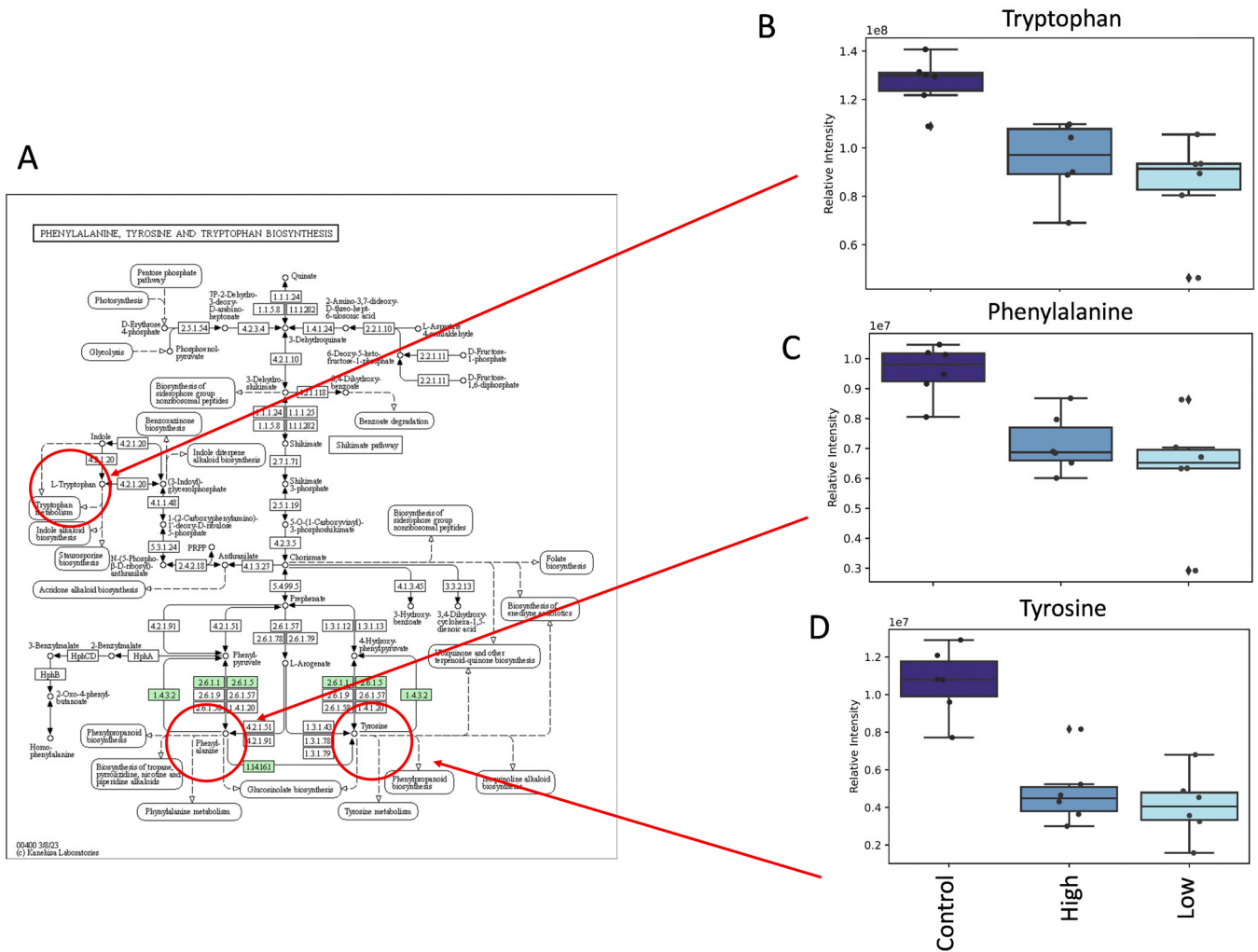


**Fig. 5.** The effects of prolonged  $H_2S$  exposure on the phenylalanine, tyrosine and tryptophan biosynthesis. **A)** The KEGG pathway, showing the three metabolites affected by  $H_2S$  regardless of the concentration. The pathway map was downloaded from KEGG PATHWAY Database (<https://www.genome.jp/kegg/pathway.html>). Relative levels of the **B)** tryptophan, **C)** phenylalanine and **D)** tyrosine in the plasma. The levels in the low and high groups were significantly lower than in the control group. The four presented elements are the median (line inside the box), the 25%–75% quartiles (the coloured box), the 9%–91% quartiles (black sticks) and individual data points (dots).

these pathways were Glycine, serine, and threonine metabolism; Thiamine metabolism; Taurine and hypotaurine metabolism; and purine metabolism.

Subsequently, alterations in individual metabolites unique to specific  $H_2S$ -exposed groups were scrutinised, as illustrated with representative level 1 metabolites in Fig. 6. The plasma levels of betaine, guanaine, and thiamine displayed significant reductions within the low group compared to the control (Fig. 6A–C). Conversely, within the high group, the levels of adenine and choline exhibited elevation, while hypoxanthine levels were lower relative to the control group (Fig. 6D–F).

### 3.4.2. Skin mucus

A total of 799 compounds were detected within the skin mucus (Fig. 7A, Supplementary File 6), and their annotations are categorised as follows: 26 metabolites were classified at level 1, 52 at level 2a, 32 compounds at level 2b, and 146 compounds were attributed to level 3. Among them, 543 compounds could be discerned from the background but lacked definitive annotations, thus remaining unknown. The score plot stemming from a PCA model, calculated on the compounds annotated at levels 1 and 2a within the reduced dataset, is showcased in Fig. 7B. This plot showcases a distinct separation among the groups, with notable variability observed in the control group in contrast to the

two  $H_2S$ -exposed groups. The loading plot (Fig. 7C) delineates the variables accountable for the patterns observed in the score plot.

Upon conducting multiple pairwise comparisons, only one metabolite exhibited a significant alteration due to  $H_2S$  exposure. Specifically, the level of 4-hydroxyproline in the skin mucus was markedly lower within the low group when compared to the control group (Fig. 7D). However, no significant disparity was observed in the levels between both  $H_2S$ -exposed groups. Remarkably, 4-hydroxyproline emerged as a metabolite significantly modified in the plasma, irrespective of the  $H_2S$  concentration (Fig. 7E).

## 4. Discussion

Recent years have witnessed Norwegian salmon farms experiencing mass mortality events linked to  $H_2S$ . Although mortality at elevated levels is extensively documented, the physiological responses to prolonged exposure to low concentrations have remained enigmatic. This study illuminates the physiological implications of a 4-week exposure to  $H_2S$  concentrations previously deemed sub-lethal. Evidently,  $H_2S$  poses health and welfare risks for salmon, as extended exposure triggers alterations from organismal to molecular levels. While these changes underscore the inherent risks, the identified molecules, and processes



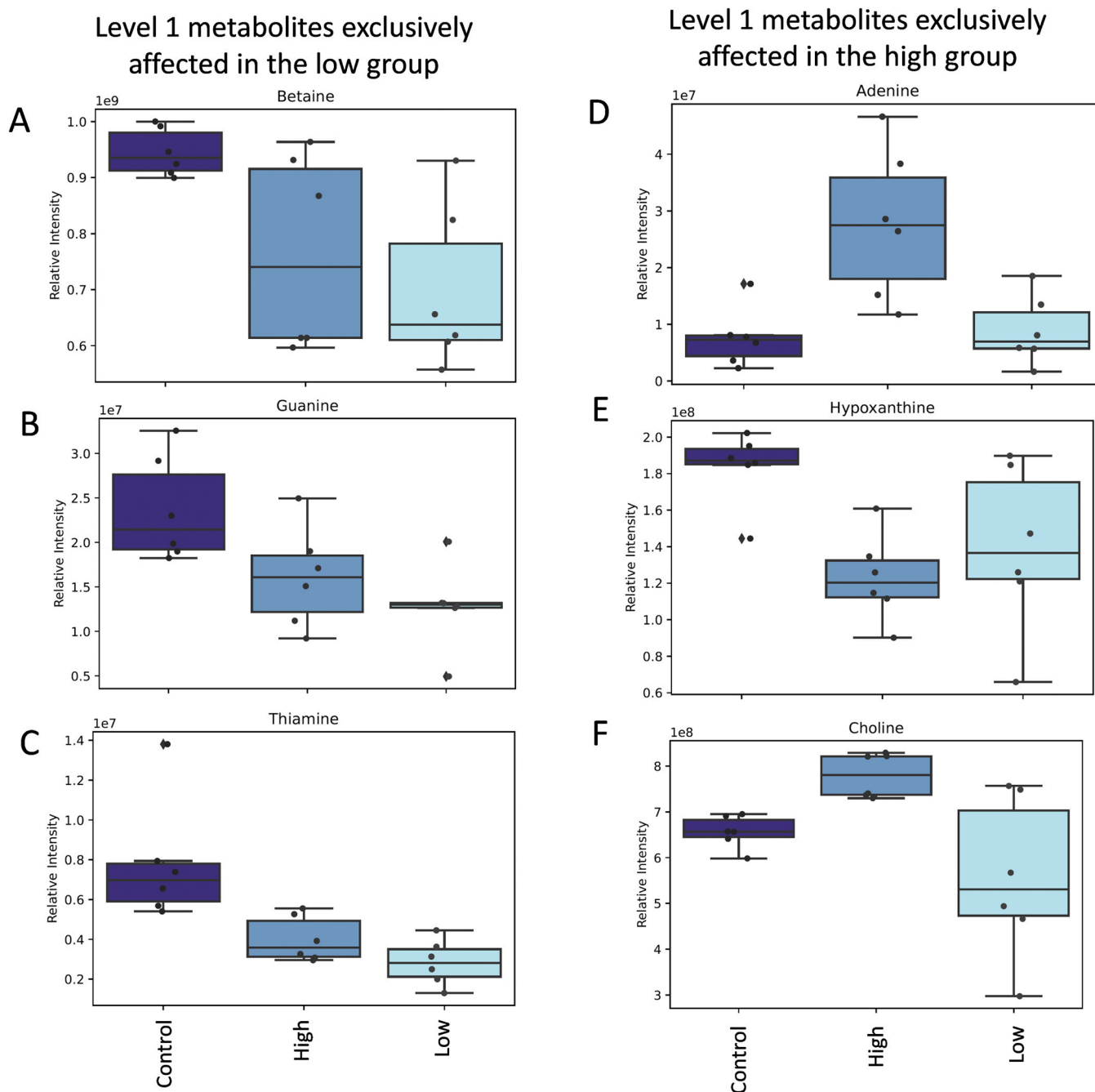


**Fig. 6.** Level 1 metabolites exclusively affected in the plasma of a particular  $H_2S$ -exposed group. **A)** betaine, **B)** guanine and **C)** thiamine were the level 1 metabolites significantly altered only in the low group. On the other hand, **D)** adenine, **E)** hypoxanthine, and **F)** choline were the level 1 metabolites that were significantly altered only in the high group. See Fig. 5 for additional information about the visualisation of the data.

responsive to  $H_2S$  shed light on the salmon's mobilisation of an array of defence molecules to defend itself from the environmental threat posed by  $H_2S$ .

#### 4.1. Prolonged $H_2S$ exposure is a welfare risk

A dose-dependent mortality was documented within the treatment groups, with the high-dose group exhibiting the highest cumulative mortality rate of 16 % following a 4-week exposure period. The 96-h LC50 of  $H_2S$  for various marine species is reported to range between 50–500  $\mu\text{g/L}$  (Boyd, 2014). However, among salmon farmers there is a shared understanding that  $H_2S$  levels should remain below 5  $\mu\text{g/L}$  in marine systems (Juel, 2020). The notion that  $H_2S$  concentrations and

tolerance levels may have been overestimated in the literature, is not uncommon. A recent study by Bergstedt and Skov (2023) demonstrated that the critical  $H_2S$  threshold for salmon smolts is considerably lower than previously assumed (Kierner et al., 1995).

While the 5  $\mu\text{g/L}$  threshold might denote a sub-lethal level during acute exposure, it could lead to lethality, characterised by progressive mortality during prolonged exposure. Notably, instances of mortality were solely observed beginning in the third week. This observation implies that during the initial two weeks, the fish were likely actively deploying countermeasures until their defences depleted and exhausted. This, in turn, heightened their susceptibility to  $H_2S$  toxicity. Partially supporting this, transcriptome data revealed greater change during the fourth week compared to the second week (Section 4.3). We proposed

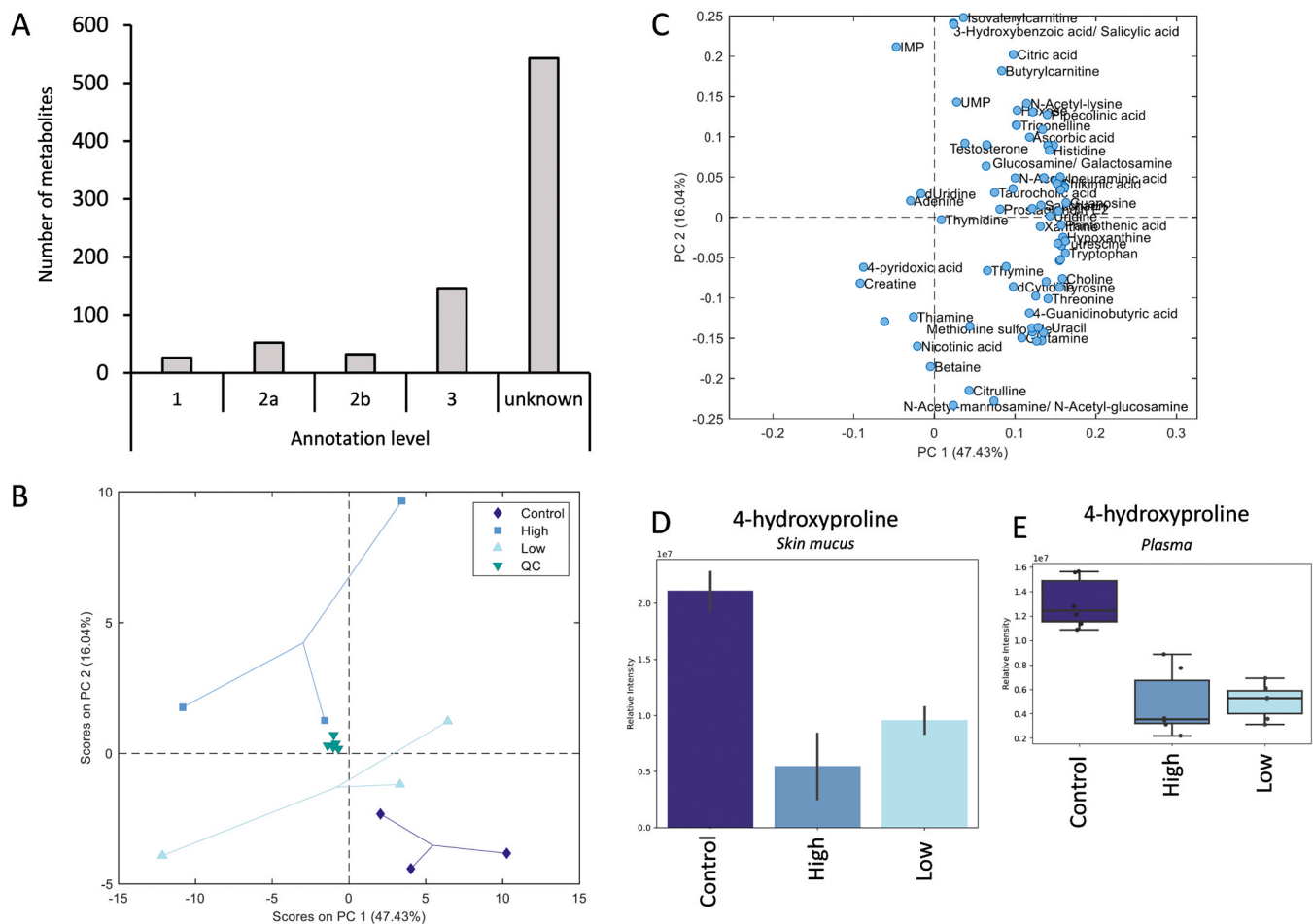


**Fig. 7.** Skin mucus metabolome of salmon following prolonged exposure to H<sub>2</sub>S. **A)** Metabolites identified in the matrix based on five annotation levels. **B)** Score plot of PC2 over PC1 in the model calculated on the relative concentrations of the variables annotated on levels 1 and 2a in the reduced dataset. **C)** Loading plot from PCA model calculated on the relative concentrations of the variables annotated on levels 1 and 2a in the reduced dataset. Refer to Fig. 5 for additional information about the plots. 4-hydroxyproline was the metabolite significantly affected by H<sub>2</sub>S exposure in both **D)** skin mucus and **E)** plasma. Each bar represents one treatment group for skin mucus, with the error bars displaying the standard deviation. See Fig. 5 for additional information about the visualisation of the plasma data. Due to limited amount, 3 fish from each RAS unit were pooled. Each treatment group represented n = 3 pooled samples.

that H<sub>2</sub>S concentrations should not exceed 1 µg/L in a salmon brackish water RAS to avert progressive mortality.

Prolonged exposure to H<sub>2</sub>S had discernible impacts on performance indicators such as weight and condition factor, highlighting the manifestation of chronic stress and its adverse repercussions on the tertiary stress responses of salmon (Barton, 2002). Recent reports indicated that salmon previously subjected to H<sub>2</sub>S exposure exhibited an impaired ability to respond to secondary stressors, underscoring the enduring effects of exposure history on allostatic load (Nicolaysen et al., 2024).

Both H<sub>2</sub>S-exposed groups demonstrated lower mean weights at the end of the trial, revealing the direct influence of extended exposure on the growth performance of salmon smolts. A parallel outcome of reduced growth after prolonged H<sub>2</sub>S exposure was noted in Bluegill (*Lepomis macrochirus*) (Smith Jr. et al., 1976) and fathead minnows (*Pimephales promelas*) (Smith, 1976). However, this growth effect contradicted an earlier study on salmon, wherein the disparity between control and H<sub>2</sub>S-treated groups was minimal (Kierner et al., 1995). This discrepancy could be attributed to the actual H<sub>2</sub>S levels the fish were exposed to, a variable the previous report failed to address adequately. The transcriptomic and histological changes in the olfactory organ following exposure might shed light on the effects of H<sub>2</sub>S on growth. We speculate that these changes affected olfaction, thereby influencing the decisive function on food procurement. On the other hand, energy allocation is common in response to toxin-related stress. It could also be

possible that the energy for growth was re-allocated for fuelling physiological countermeasures against H<sub>2</sub>S. This was partly supported by systemic changes in metabolome (Section 4.4).

The influence on diminished growth at elevated levels was also recorded in essential water quality parameters within the RAS, including carbon dioxide (Khan et al., 2018) and nitrite (Gutiérrez et al., 2019). This underscores the significance of rearing conditions in controlled systems for optimising fish performance. Beyond the threat of mortality, elevated H<sub>2</sub>S levels during salmon rearing can predictably lead to stunted growth. The condition factor (K) indicates the relative resilience and overall well-being of fish. Our observations revealed that prolonged H<sub>2</sub>S exposure could adversely affect this parameter, specifically within the low-dose group. Despite this inter-group variance, the K values for all groups remain within the acceptable range for smolts.

#### 4.2. Structural features of the olfactory organ are altered by prolonged H<sub>2</sub>S exposure

The nasal passages exposed to airborne irritants are susceptible to toxicant-induced damage (Shusterman, 2003). Accordingly, terrestrial vertebrate evidence has highlighted pronounced sensitivity to H<sub>2</sub>S of the olfactory epithelium (ACGIH, 1986; Breneman et al., 2002). Our prior work utilising *in vitro* and *ex vivo* models demonstrated that H<sub>2</sub>S (via a sulphide donor) impacts the olfactory organ of salmon (Alipio et al.,

2022; Cabillon and Lazado, 2022). This finding was corroborated by an *in vivo* acute exposure study that showcased H<sub>2</sub>S-induced alterations in the nasal mucosa structures of salmon, albeit in a mild manner (Alipio et al., 2023).

In our current study, we have revealed that prolonged exposure to H<sub>2</sub>S can lead to damage within the olfactory epithelium of the nasal mucosa. This phenomenon became evident during the fourth week, even though a dose-dependent response was not discernible. These phenotypic changes support the transcriptomic data, where genes associated with the extracellular matrix, including the large collagen group, displayed susceptibility to the effects of H<sub>2</sub>S exposure. In mammals, exposure to H<sub>2</sub>S has been linked to olfactory neuronal loss and basal cell hyperplasia, often accompanied by epithelial damage that may result in bleeding (Mousa, 2015). While we did not document such drastic changes in our study, it is conceivable that H<sub>2</sub>S could moderately influence mucosal structure at the concentrations tested.

Oedema-like vacuoles were observed primarily in the lamellar tip, particularly in fish exposed to 5 µg/L. In human studies, pulmonary oedema has been recognised as a prominent outcome of prolonged H<sub>2</sub>S toxicity, causing excessive accumulation of interstitial fluid and detrimentally affecting tissue function by impeding the diffusion of oxygen and essential nutrients, thereby compromising cellular metabolism (Guidotti, 2010; Scallan et al., 2010). The emergence of these oedema-like vacuoles in our observations coincided with the fourth week, a timeframe aligning with the potential depletion of the countermeasures against H<sub>2</sub>S. Whether this pathology persists over an extended duration and contributes to heightened mortality rates at elevated concentrations warrants further investigation. It is plausible to speculate that their heightened presence at higher H<sub>2</sub>S levels implies a compromised local cellular metabolism, subsequently influencing the efficient diffusional removal of potentially toxic compounds.

Mucus cells, responsible for producing the glycomic viscous substance that lines the mucosa, serve as a biological and physical barrier against environmental threats. Our findings revealed an increased density of mucus cells in the epithelia of the lamella and nasal wall, aligning with previous evidence indicating that mucus secretion indeed plays a protective role against the potent mucosal irritant that is H<sub>2</sub>S (Alipio et al., 2022; Motta et al., 2015).

#### 4.3. H<sub>2</sub>S modifies the transcriptomic landscape of the olfactory organ

Transcriptomic analysis of the olfactory organ unequivocally demonstrated that the extent of alterations was profoundly influenced by both the duration of exposure and the concentration of H<sub>2</sub>S. Remarkably significant changes emerged within the nasal transcriptome of the high-exposure group during the fourth week, a timing that notably aligned with the observation of structural transformations within the olfactory organ. The observed alterations in the nasal transcriptome are in congruence with previous transcriptome-wide investigations that unveiled the olfactory epithelium's capacity to orchestrate a comprehensive molecular response to H<sub>2</sub>S, and these molecular changes can be mirrored phenotypically (Roberts et al., 2008).

Functioning as a barrier separating internal and external environments, the epithelium of the fish mucosa is directly exposed to environmental toxicants. Of note, a substantial cluster of genes predominantly demonstrated downregulation, primarily within the extracellular matrix (ECM). The ECM is an intricate network composed of multifaceted macromolecules intricately linked to form a mechanically robust composite, contributing indispensably to the mechanical properties of tissues (Yue, 2014). In the context of fish mucosa, the significance of ECM is pivotal for its defensive functions. Consequently, the downregulation of these genes within the olfactory organ of H<sub>2</sub>S-exposed fish signals that this environmental toxicant impairs the mucosa by compromising the molecules essential for upholding its structural integrity, thereby undermining its functional capacity.

Collagen, a sizeable family of proteins, assumes central structural

roles and significantly contributes to tissues mechanical attributes, architecture, and form (Ricard-Blum, 2011). Most of the ECM-related genes that experienced downregulation in response to H<sub>2</sub>S exposure belonged to the collagen family, particularly the collagen type 1 group, a prevalent collagen molecule in teleosts (Gistelink et al., 2016). Another cluster of genes adversely affected by H<sub>2</sub>S pertains to membrane-bound mucins – specifically, *mucin 17* and *mucin 22*. These non-gel-forming mucins play a critical role in mediating cell–cell and cell–extracellular matrix interactions while functioning as receptors and sensors to facilitate signal transduction in epithelial cells (Lin et al., 2021). Furthermore, H<sub>2</sub>S-exposed fish exhibited downregulation of additional ECM proteins, including *laminin*, *fibronectin*, *spondin*, and *GMP giant mucus protein*. While these proteins fulfil distinct functions, their roles often intersect to ensure tissue homeostasis, facilitate tissue repair, regulate cell attachment and motility, and sustain barrier integrity (Agha-Mir-Salim et al., 1993; Deroo and Cudmore, 2011; Meng et al., 2013). The compromise of the mucosal barrier is a detrimental consequence of prolonged H<sub>2</sub>S exposure, shedding light on its potential mucosal immunotoxicity.

H<sub>2</sub>S encompasses immunological functions, impacting mediators of both innate immunity—such as neutrophils, macrophages, dendritic cells, natural killer cells, mast cells, basophils, and eosinophils—and adaptive immunity encompassing T and B lymphocytes (Dilek et al., 2020). Beyond its role in olfaction, the olfactory organ of fish houses the nasopharynx-associated lymphoid tissue, a key player in mucosal immunity (Lazado et al., 2023). In a previous study, we unveiled that nasal leukocytes from the olfactory organ of salmon mount robust immune responses to H<sub>2</sub>S, affecting pathways of both branches of immunity (Cabillon and Lazado, 2022). Our current study corroborates these findings, demonstrating that prolonged H<sub>2</sub>S exposure gives rise to an elevated immunological state within the olfactory organ, possibly forming part of the defence mechanism against the threats posed by H<sub>2</sub>S. This immunomodulatory role of H<sub>2</sub>S was evident in a concentration-dependent manner, with the high-exposure group displaying a more pronounced response.

Remarkably, our observations revealed an upregulation of genes associated with viral immunity in H<sub>2</sub>S-exposed fish. To our knowledge, this phenomenon has not been previously demonstrated in teleost fish. Nonetheless, our data align with earlier evidence in mammals that highlight the antiviral function of H<sub>2</sub>S within airway mucosa (Citi et al., 2020; Ivanciuc et al., 2016), suggesting a potentially common evolutionary response among animals. Specifically, genes from the Tripartite motif (TRIM) family, such as TRIM-5, TRIM-7, and TRIM-11, exhibited substantial impacts due to H<sub>2</sub>S exposure. TRIM proteins constitute a prominent family of E3 ubiquitin ligases and have been implicated in innate immunity, inflammation, and virus replication (Giraldo et al., 2020; Yang et al., 2020), a concept extending to fish, albeit with limited comprehension (Langevin et al., 2019). The interplay between TRIM proteins and H<sub>2</sub>S remains uncharted territory. Given that TRIM mediates inflammation (Uchil et al., 2013) and H<sub>2</sub>S can trigger robust inflammatory responses (Dilek et al., 2020), we hypothesise that TRIM proteins tightly orchestrate the inflammatory response to H<sub>2</sub>S within the olfactory organ, ensuring the precision of the response mechanism.

#### 4.4. Metabolomics provide insights into the systemic impacts of prolonged H<sub>2</sub>S exposure

In a previous acute exposure trial conducted at significantly higher concentrations, we observed that the impact of H<sub>2</sub>S exposure on the metabolome of skin mucus was more pronounced than on blood in salmon smolts. This underscored that transient H<sub>2</sub>S exposure primarily affected the mucosa rather than the systemic level (Alipio et al., 2023). However, in the present study, we identified a distinct profile where H<sub>2</sub>S-induced changes were more prominent in plasma than skin mucus. Disparities in concentrations, exposure durations, and salinity conditions (seawater at 35 ppt in the study by (Alipio et al., 2023)) could serve

as plausible explanations for these variations. Nonetheless, an alternative explanation could be that acute exposure triggered a heightened mucosal response due to the necessity for an immediate reaction, whereas prolonged exposure might have elicited a more gradual response, allowing for a comprehensive system-wide mobilisation to counteract the effects of H<sub>2</sub>S. We believe that these systemic physiological changes contribute to reduced growth and mortality as the alterations in key metabolite levels such as nucleosides and amino acids suggest changes in energy metabolism (Wang et al., 2023). Interestingly, we observed a greater number of significantly altered plasma metabolites in the low-exposure group than the high-exposure group, suggesting that a linear relationship to concentration did not govern the impact.

Our investigation concentrated on metabolites impacted by H<sub>2</sub>S, irrespective of concentration, specifically identifying the core pathways affected. These pivotal pathways encompass phenylalanine, tyrosine, and tryptophan biosynthesis; phenylalanine metabolism; Aminoacyl-tRNA biosynthesis; Glycine, serine, and threonine metabolism; Riboflavin metabolism, and D-Glutamine and D-glutamate metabolism. Aromatic amino acids – phenylalanine, tyrosine, and tryptophan – belong to the class of  $\alpha$ -amino acids, participating ubiquitously in protein synthesis, while their secondary metabolites hold significant roles linked to health and defence against both biotic and abiotic stresses (Parthasarathy et al., 2018). Interestingly, the levels of phenylalanine, tryptophan, and tyrosine were substantially diminished in the plasma of H<sub>2</sub>S-exposed fish. Phenylalanine and tryptophan are amino acids that fish cannot synthesise and are typically obtained through diet. One conceivable explanation for the reduced levels of phenylalanine and tryptophan could be that the stress instigated by H<sub>2</sub>S potentially hindered the fish ability to assimilate these crucial amino acids. It is well-documented that stressful conditions impact amino acid metabolism and requirements in fish (Aragão et al., 2008; Costas et al., 2008). Conversely, tyrosine is pivotal in stress responses, serving as a precursor for hormones and neurotransmitters, including epinephrine, norepinephrine, and dopamine (Herrera et al., 2019). The levels of these metabolites in fish have been observed to increase during periods of stress (Costas et al., 2008). However, our study documented a reduction in tyrosine levels, indicating that H<sub>2</sub>S likely interfered with this crucial stress response mechanism. This lends support to an earlier observation that prolonged exposure to H<sub>2</sub>S affected the stress responses to a secondary stressor in salmon (Nicolaysen et al., 2024).

Structural integrity of collagen relies heavily on proline and its principal hydroxylated variant, 4-hydroxyproline (Taga et al., 2021). Intriguingly, we uncovered that 4-hydroxyproline emerged as a shared metabolite in both plasma and skin mucus, and its levels were markedly diminished in groups subjected to H<sub>2</sub>S exposure. This revelation could further illuminate into the repercussions of H<sub>2</sub>S on the extracellular matrix, particularly concerning collagens within the olfactory organ. In a study involving a mammalian myocardial fibrosis model, the sulphide donor GYY4137 demonstrated the capability to decrease hydroxyproline concentration, concurrently leading to shifts in collagen expression (Meng et al., 2015). The distinctive response patterns of 4-hydroxyproline within plasma and skin mucus imply that it might serve as a prominent target of H<sub>2</sub>S and warrant further exploration as a potential marker for assessing the response of salmon to H<sub>2</sub>S. On the other hand, higher hydroxyproline was documented to enhance salmon growth (Aksnes et al., 2008). We speculate that the decrease in 4-hydroxyproline in both matrices affected the growth potential of H<sub>2</sub>S-exposed fish, thus, lower weight gain and condition factor were documented.

Several metabolites exhibit the potential to serve as markers for H<sub>2</sub>S toxicity, as their changes were distinctly influenced by concentration. Adenine, guanine, and thiamine, three of the four nitrogenous bases constituting the fundamental building blocks of DNA, showed alterations in their plasma levels due to H<sub>2</sub>S exposure. These shifts might hint at H<sub>2</sub>S interfering with DNA synthesis. In particular, H<sub>2</sub>S is known to modulate DNA stability, yielding varied outcomes contingent on different concentrations and exposure durations (Shackelford et al.,

2021).

Hypoxanthine, regarded as an essential stress metabolite checkpoint, governs energy metabolism within cells (Lee et al., 2018). In a previous study, we documented an increase in its levels in the skin mucus of salmon following transient exposure to H<sub>2</sub>S (Alipio et al., 2023). Yet, in the current investigation, we observed a decrease in hypoxanthine levels in plasma, suggesting that prolonged exposure might have constrained its production. Despite this disparity, it remains intriguing to explore how this metabolite behaves across diverse biological matrices under varying H<sub>2</sub>S scenarios.

#### 4.5. Conclusion

This study presents compelling evidence that prolonged exposure to elevated H<sub>2</sub>S levels poses a substantial health and welfare risk to Atlantic salmon. While mortality is a well-documented outcome associated with elevated H<sub>2</sub>S levels, the intricate physiological alterations underpinning this result remain underexplored. This study takes a significant step forward by demonstrating that extended H<sub>2</sub>S exposure can curtail production performance and provoke significant modifications in the transcriptome and metabolome of salmon. The susceptibility of the olfactory organ to H<sub>2</sub>S was highlighted by discernible albeit modest structural changes. Furthermore, the transcriptome data unveiled the perturbation of genes crucial for extracellular matrix integrity and immunity, accentuating the immunotoxicity towards mucosal barrier functions. Metabolomics shed illuminating insights into the systemic repercussions of H<sub>2</sub>S, exposing its interference with amino acid metabolism and synthesis.

These findings contribute substantially to augmenting our understanding of the biological ramifications of environmental H<sub>2</sub>S exposure, a knowledge base that could prove pivotal in devising effective strategies for mitigating this threat within salmon land-based aquaculture.

#### CRediT authorship contribution statement

**Megård Reiten Britt Kristin:** Writing – review & editing, Writing – original draft, Methodology, Investigation. **Timmerhaus Gerrit:** Writing – review & editing, Writing – original draft, Visualization, Validation, Software, Resources, Methodology, Data curation. **Nicolaysen Iona Lorraine:** Writing – review & editing, Writing – original draft, Methodology, Investigation. **Alipio Hanna Ross D:** Writing – review & editing, Writing – original draft, Methodology, Investigation. **Carletto Danilo:** Writing – review & editing, Writing – original draft, Methodology, Investigation. **Andersen Øivind:** Writing – review & editing, Writing – original draft, Investigation, Formal analysis, Conceptualization. **Hansen Bergstedt Julie:** Writing – review & editing, Writing – original draft, Supervision, Resources, Methodology, Investigation, Formal analysis. **Stiller Kevin T:** Writing – review & editing, Writing – original draft, Supervision, Resources, Methodology, Investigation, Formal analysis. **Lazado Carlo C:** Writing – review & editing, Writing – original draft, Visualization, Validation, Supervision, Project administration, Methodology, Investigation, Funding acquisition, Formal analysis, Data curation, Conceptualization.

#### Declaration of Competing Interest

The authors declare that they have no known competing financial interests or personal relationships that could have appeared to influence the work reported in this paper.

#### Data Availability

Accession number of microarray data is provided in the text. Additional data are provided as Supplementary Materials.



## Acknowledgements

This study received funding from the Research Council of Norway (H2Salar, ref. 300825). HR Alipio and D Carletto thank European Commission's Erasmus programme for financing their research stay at Nofima. We would like to thank Yuriy Marchenko for the assistance in the *in vivo* trial, Åse Åtland and Paulo Fernandes of NIVA for the H<sub>2</sub>S dosing advice, Eldar Lien of SeaRAS for the technical help in H<sub>2</sub>S measurement, and Aleksei Krasnov, Marianne Hansen and Marianne Vaadal for the microarray analysis. Thorsten Gravert is also thanked for his assistance in metabolomics.

## Appendix A. Supporting information

Supplementary data associated with this article can be found in the online version at [doi:10.1016/j.ecoenv.2023.115897](https://doi.org/10.1016/j.ecoenv.2023.115897).

## References

- ACGIH, H., Documentation of the threshold limit values and biological exposure indices. American Conference of Governmental Industrial Hygienists, Vol. 5, 1986, pp. 50–52.
- Agha-Mir-Salim, P., et al., 1993. Electron and fluorescence microscopic investigations on composition and structure of the epithelial basement membrane of the human inferior nasal concha. *Eur. Arch. Oto-Rhino-Laryngol.* 250, 401–407.
- Ahmed, N., Turchini, G.M., 2021. Recirculating aquaculture systems (RAS): environmental solution and climate change adaptation. *J. Clean. Prod.* 297, 126604.
- Aksnes, A., et al., 2008. The effect of dietary hydroxyproline supplementation on salmon (*Salmo salar* L.) fed high plant protein diets. *Aquaculture* 275, 242–249.
- Alipio, H.R.D., et al., 2022. Sulphide donors affect the expression of mucin and sulphide detoxification genes in the mucosal organs of Atlantic salmon (*Salmo salar*). *Front. Physiol.* 13, 1083672.
- Alipio, H.R.D., et al., 2023. Differential sensitivity of mucosal organs to transient exposure to hydrogen sulphide in post-smolt Atlantic salmon (*Salmo salar*). *Aquaculture* 573, 739595.
- Aragão, C., et al., 2008. Stress response and changes in amino acid requirements in Senegalese sole (*Solea senegalensis* Kaup 1858). *Amino Acids* 34, 143–148.
- Badiola, M., et al., 2012. Recirculating Aquaculture Systems (RAS) analysis: main issues on management and future challenges. *Aquac. Eng.* 51, 26–35.
- Bagarinao, T., 1992. Sulphide as an environmental factor and toxicant: tolerance and adaptations in aquatic organisms. *Aquat. Toxicol.* 24, 21–62.
- Bagarinao, T., Vetter, R.D., 1989. Sulphide tolerance and detoxification in shallow-water marine fishes. *Mar. Biol.* 103, 291–302.
- Barton, B.A., 2002. Stress in fishes: a diversity of responses with particular reference to changes in circulating corticosteroids. *Integr. Comp. Biol.* 42, 517–525.
- Bergstedt, J.H., Skov, P.V., 2023. Acute hydrogen sulfide exposure in post-smolt Atlantic salmon (*Salmo salar*): critical levels and recovery. *Aquaculture* 570, 739405.
- Bjørndal, T., Tusvik, A., 2019. Economic analysis of land based farming of salmon. *Aquac. Econ. Manag.* 23, 449–475.
- Boyd, C.E., 2014. Hydrogen sulfide, toxic but manageable. *Glob. Aquac. Advocate* 34–36.
- Brenneman, K.A., et al., 2002. Olfactory mucosal necrosis in male CD rats following acute inhalation exposure to hydrogen sulfide: reversibility and the possible role of regional metabolism. *Toxicol. Pathol.* 30, 200–208.
- Cabillon, N.A.R., Lazado, C.C., 2022. Exogenous sulphide donors modify the gene expression patterns of Atlantic salmon nasal leukocytes. *Fish. Shellfish Immunol.* 120, 1–10.
- Citi, V., et al., 2020. Anti-inflammatory and antiviral roles of hydrogen sulfide: Rationale for considering H<sub>2</sub>S donors in COVID-19 therapy. *Br. J. Pharm.* 177, 4931–4941.
- Costas, B., et al., 2008. High stocking density induces crowding stress and affects amino acid metabolism in Senegalese sole *Solea senegalensis* (Kaup 1858) juveniles. *Aquac. Res.* 39, 1–9.
- Deroo, B.J., Cudmore, C.S., 2011. The extracellular matrix protein, spondin 1, regulates proliferation, survival, and adhesion of granulosa cells. *Biol. Reprod.* 85, 701–701.
- Dilek, N., et al., 2020. Hydrogen sulfide: an endogenous regulator of the immune system. *Pharm. Res* 161, 105119.
- Doneanu, C.E., et al., 2011. UPLC/MS monitoring of water-soluble vitamin Bs in cell culture media in minutes. *Water Application Note.* 720004042en.
- Giraldo, M.I., et al., 2020. TRIM proteins in host defense and viral pathogenesis. *Curr. Clin. Microbiol. Rep.* 7, 101–114.
- Gistelincq, C., et al., 2016. Zebrafish collagen type I: molecular and biochemical characterization of the major structural protein in bone and skin. *Sci. Rep.* 6, 21540.
- Guidotti, T.L., 2010. Hydrogen sulfide: advances in understanding human toxicity. *Int. J. Toxicol.* 29, 569–581.
- Gutiérrez, X.A., et al., 2019. Effects of chronic sub-lethal nitrite exposure at high water chloride concentration on Atlantic salmon (*Salmo salar*, Linnaeus 1758) parr. *Aquac. Res.* 50, 2687–2697.
- Harada, H., et al., 1994. Interaction between sulfate-reducing bacteria and methane-producing bacteria in UASB reactors fed with low strength wastes containing different levels of sulfate. *Water Res.* 28, 355–367.
- Herrera, M., et al., 2019. The use of dietary additives in fish stress mitigation: comparative endocrine and physiological responses. *Front. Endocrinol. (Lausanne)* 10, 447.
- Ivančić, T., et al., 2016. Hydrogen sulfide is an antiviral and anti-inflammatory endogenous gasotransmitter in the airways: role in respiratory syncytial virus infection. *Am. J. Respir. Cell Mol. Biol.* 55, 684–696.
- Juel, H.H., Solving the problem of hydrogen sulfide on a fish farm. *Innovation News Network Online* 2020.
- Khan, J.R., et al., 2018. The effects of acute and long-term exposure to CO<sub>2</sub> on the respiratory physiology and production performance of Atlantic salmon (*Salmo salar*) in freshwater. *Aquaculture* 491, 20–27.
- Kierner, M.C.B., et al., 1995. The effects of chronic and acute exposure to hydrogen sulphide on Atlantic salmon (*Salmo salar* L.). *Aquaculture* 135, 311–327.
- Krasnov, A., et al., 2011. Development and assessment of oligonucleotide microarrays for Atlantic salmon (*Salmo salar* L.). *Comp. Biochem. Physiol. Part D: Genom. Proteom.* 6, 31–38.
- Langevin, C., et al., 2019. Fish antiviral tripartite motif (TRIM) proteins. *Fish. Shellfish Immunol.* 86, 724–733.
- Lazado, C.C., et al., 2020. Oxidant-induced modifications in the mucosal transcriptome and circulating metabolome of Atlantic salmon. *Aquat. Toxicol.* 227, 105625.
- Lazado, C.C., et al., 2021. Multiomics provide insights into the key molecules and pathways involved in the physiological adaptation of Atlantic salmon (*Salmo salar*) to chemotherapeutic-induced oxidative stress. *Antioxidants* 10, 1931.
- Lazado, C.C., et al., 2023. Comparative basal transcriptome profiles of the olfactory rosette and gills of Atlantic salmon (*Salmo salar*) unveil shared and distinct immunological features. *Genomics* 115, 110632.
- Lazado, C.C., Good, C., 2021. Survey findings of disinfection strategies at selected Norwegian and North American land-based RAS facilities: a comparative insight. *Aquaculture* 532, 736038.
- Lee, J.S., et al., 2018. Hypoxanthine is a checkpoint stress metabolite in colonic epithelial energy modulation and barrier function. *J. Biol. Chem.* 293, 6039–6051.
- Letelier-Gordo, C.O., et al., 2020. Increased sulfate availability in saline water promotes hydrogen sulfide production in fish organic waste. *Aquac. Eng.* 89, 102062.
- Lien, E., et al., 2022. The SeaRAS AquaSense™ System: real-time monitoring of H<sub>2</sub>S at Sub µg/L levels in recirculating aquaculture systems (RAS). *Front. Mar. Sci.* 9.
- Lin, S., et al., 2021. Differential *MUC22* expression by epigenetic alterations in human lung squamous cell carcinoma and adenocarcinoma. *Oncol. Rep.* 45, 78.
- Meng, G., et al., 2015. Hydrogen sulfide donor GYY4137 protects against myocardial fibrosis. *Oxid. Med Cell Longev.* 2015, 691070.
- Meng, J., et al., 2013. The development of nasal polyp disease involves early nasal mucosal inflammation and remodelling. *PLoS One* 8, e82373.
- Motta, J.-P., et al., 2015. Hydrogen sulfide protects from colitis and restores intestinal microbiota biofilm and mucus production. *Inflamm. Bowel Dis.* 21, 1006–1017.
- Mousa, H.A., 2015. Short-term effects of subchronic low-level hydrogen sulfide exposure on oil field workers. *Environ. Health Prev. Med.* 20, 12–17.
- Muyzer, G., Stams, A.J.M., 2008. The ecology and biotechnology of sulphate-reducing bacteria. *Nat. Rev. Microbiol.* 6, 441–454.
- Nicolaysen, I.L., Alipio, H.R., Megård-Reiten, B.K., Stiller, K.T., Lazado, C.C., 2024. Stress and gut responses of post-smolt Atlantic salmon (*Salmo salar*) to elevated levels of hydrogen sulphide. *Aquaculture* 581, 740467.
- Osório, J., et al., 2022. Intermittent administration of peracetic acid is a mild environmental stressor that elicits mucosal and systemic adaptive responses from Atlantic salmon post-smolts. *BMC Zool.* 7 (1), 17.
- Parthasarathy, A., et al., 2018. A three-ring circus: metabolism of the three proteogenic aromatic amino acids and their role in the health of plants and animals. *Front. Mol. Biosci.* 5.
- Reynolds, F.A., The effects of long-term exposure to low concentrations of hydrogen sulphide on brown trout, *Salmo trutta*. S. U. N. Y. College at Brockport., 1976.
- Ricard-blum, S., 2011. The collagen family. *Cold Spring Harb. Perspect. Biol.* 3, a004978.
- Roberts, E.S., et al., 2008. Gene expression changes following acute hydrogen sulfide (H<sub>2</sub>S)-induced nasal respiratory epithelial injury. *Toxicol. Pathol.* 36, 560–567.
- Rojas-Tirado, P., et al., 2021. Biofilters are potential hotspots for H<sub>2</sub>S production in brackish and marine water RAS. *Aquaculture* 536, 736490.
- Scallan, J., et al., Integrated Systems Physiology: from Molecule to Function to Disease. Capillary Fluid Exchange: Regulation, Functions, and Pathology. Morgan & Claypool Life Sciences Copyright © 2010 by Morgan & Claypool Life Sciences., San Rafael (CA), 2010.
- Shackelford, R., et al., 2021. Hydrogen sulfide and DNA repair. *Redox Biol.* 38, 101675.
- Shusterman, D., 2003. Toxicology of nasal irritants. *Curr. Allergy Asthma Rep.* 3, 258–265.
- Smith, L., et al., 1977. The effect of methemoglobin on the inhibition of cytochrome c oxidase by cyanide, sulfide or azide. *Biochem. Pharmacol.* 26, 2247–2250.
- Smith Jr., L., Oseid, D., 1974. Effect of hydrogen sulfide on development and survival of eight freshwater fish species. The Early Life History of Fish: The Proceedings of an International Symposium Held at the Dunstaffnage Marine Research Laboratory of the Scottish Marine Biological Association at Oban, Scotland, from May 17–23, 1973. Springer., pp. 417–430.
- Smith, L.L., 1976. Effect of Hydrogen Sulfide on Fish and Invertebrates: Acute and chronic toxicity studies. US Environmental Protection Agency, Office of Research and Development ....
- Smith Jr., L.L., et al., 1976. Toxicity of hydrogen sulfide to various life history stages of Bluegill (*Lepomis macrochirus*). *Trans. Am. Fish. Soc.* 105, 442–449.
- Taga, Y., et al., 2021. In-depth correlation analysis demonstrates that 4-hydroxyproline at the Yaa position of Gly-Xaa-Yaa repeats dominantly stabilizes collagen triple helix. *Matrix Biol.* 10, 100067.



- Uchil, P.D., et al., 2013. TRIM protein-mediated regulation of inflammatory and innate immune signaling and its association with antiretroviral activity. *J. Virol.* 87, 257–272.
- Wang, F., et al., 2023. Plasma metabolomic profiles associated with mortality and longevity in a prospective analysis of 13,512 individuals. *Nat. Commun.* 14, 5744.
- Xia, J., et al., 2009. MetaboAnalyst: a web server for metabolomic data analysis and interpretation. *Nucleic Acids Res.* 37, W652–W660.
- Yang, W., et al., 2020. To TRIM the immunity: from innate to adaptive immunity. *Front. Immunol.* 11.
- Ytrestøyl, T., et al., 2020. Performance and welfare of Atlantic salmon, *Salmo salar* L. post-smolts in recirculating aquaculture systems: importance of salinity and water velocity. *J. World Aquac. Soc.* 51, 373–392.
- Yue, B., 2014. Biology of the extracellular matrix: an overview. *J. Glaucoma* 23, S20–S23.